 DOI: 10.3217/978-3-85125-883-7-09

CFD VALIDATION FOR TUNNEL SMOKE CONTROL DESIGN

[1]Michael Beyer, [1,2]Conrad Stacey
[1]Stacey Agnew Pty Ltd, Australia
[2]SAMJ LLC, USA

ABSTRACT

With no reliable formula for determining minimum required upstream velocity to control smoke in tunnels, attention has turned to CFD for answers. However, CFD must be used with caution, as it produces many different answers, depending on the quality of the algorithms and coding, and how parameters and numerical models are selected. It is really only valid when the whole system of analysis (analyst + software + parameter/model choices) has been validated against known and relevant real fire scenarios. If the analyst is new, the software is different, solution parameters change, or there is no real case for comparison, perhaps it can no longer be relied on. A validation of a system of analysis against the best available tunnel fire data (Memorial Tunnel tests) is presented, with discussion on how different modelling options and software can affect the outcome, leading to conclusions as to how to model smoke control in tunnels that are not so different (in the physics and flow regimes present) to the Memorial Tunnel tests. How far the techniques might be stretched to different geometries or fire scenarios is also discussed briefly.

Keywords: CFD, tunnel fire, CFD validation, smoke propagation

1. INTRODUCTION

Smoke control during a tunnel fire is an ongoing discussion, with different strategies/philosophies established in different countries by their national standards or experiences. A common approach is the 'critical velocity philosophy', where upstream propagation of a hot smoke layer is just prevented. Avoiding any onset of backlayering with sufficiently high upstream velocities causes higher smoke/air mixing, and even higher downstream velocities, due to expansion of the air/smoke mixture caused by the heat addition. Besides the smoke mixing effect, a high upstream air velocity is also likely to cause faster fire growth, a higher peak heat release rate, and greater fire spread, as concluded in [1].

In Europe, a low velocity philosophy is usually recommended, to facilitate evacuation. A lower upstream tunnel air velocity might allow some backlayering of smoke (depending on the realised heat release rate) but reduces the risk of destroying any possible smoke stratification and leads to a lower smoke propagation speed downstream of the fire. Lower velocities are more likely to support tenable escape conditions downstream of a fire.

Further discussion on different smoke control philosophies can be found in [2] and [3]. NFPA 502, the national standard in the US, which historically proposed a 'critical velocity' approach, will now change its terminology from preventing backlayering to controlling backlayering (with the 2023 edition). That change allows for some backlayering of hot smoke, especially within the zone close to a fire that can already be considered as untenable due to radiation or other risks. It will then be more aligned with the European approach. The backlayering distance which may be judged as acceptable might depend on the available clearance and space/room above tunnel users and responders for hot smoke, and on the length of the zone already made untenable by the fire.

There is currently no sufficiently accurate or reliable formula for critical velocity, see [4], let alone the "confinement" velocity required to "control" smoke in tunnels by targeting a backlayering length for a specific design fire scenario. Lacking such knowledge, attention has turned to computational fluid dynamics (CFD) for answers. However, CFD must be used with

care, as the results can vary widely, depending on the selection of parameters and numerical models. To avoid design errors and to generate reliable answers, it is necessary to validate a CFD model against at least one relevant real fire test. This paper presents a validation, for different fire heat release rates (HRR), of a CFD model using ANSYS Fluent, against the best available tunnel fire data [5], [6]. Fire Dynamics Simulator (FDS) has also been used and compared with the test data, as it is a simulation tool often used for analysing tunnel fires.

2. TEST DATA FOR VALIDATION

The Memorial Tunnel test data are the best documented full scale fire test available and were therefore selected as a base for a reliable model validation. Geometrical details and raw data of temperature sensors, velocity sensors, fuel pumping rates, change in fire pan fuel weights etc. were packed in a 9 CD set and are still publicly available [6]. The processed raw data with the comprehensive test reports, graphics, plots, pictures, videos, and test results are also summarised on a two-disc interactive CD-ROM package [5]. The information from those packages that are relevant to the CFD validation are mentioned here.

During the test program from 1993 to 1995, in total 98 fire ventilation tests were conducted, with fire sizes of 10, 20, 50 and 100 MW, and with a series of ventilation configurations including different fully and semi transverse ventilation strategies, point supply and extraction, natural ventilation, and longitudinal ventilation with jet fans. After the completion of the tests with the transverse ventilation configuration (using the central fans in the ventilation building), the false ceiling was removed, and the ventilation system was transformed into longitudinal ventilation with jet fans. The tunnel configuration and test setup after the ceiling was removed was used as the base for the CFD model validation.

Before using the test parameter data as input parameters for the CFD model, the raw data (readings of the individual sensors) have been processed according to the details given in the Memorial Tunnel Test Data Report [6] and compared with the processed and documented test data of the comprehensive test report [5] to see if the data are consistent and reliable. The reported bulk flow rates and temperatures as well as the averaged flow parameters could be reproduced, based on the documented parameters and calibration factors.

The Memorial Tunnel report [5] concluded that the most reliable measurement loop for bulk flow is Loop 214 at the northern end of the tunnel. Review for this work revealed that other loops are clearly affected by jet fan and radiation influences on the temperature correction for pitot measurements. Local upstream average velocities are calculated based on the flow rate measured at Loop 214 and the local tunnel cross sectional area.

As an example, Figure 1 illustrates the mass flow rate at the different measurement loops for test 611 (50 MW pan fire) at three different times (89 s, 59 s and 29 s) before ignition (0 s) when there were no jet fans running and flow was being driven by a natural pressure difference, and at several time stamps after ignition (from 856 s to 976 s) when both jet fans and heat were affecting readings.

That plot shows that the mass flow rate before ignition (at cold flow) is nearly constant, as it must be by continuity. However, after ignition, the reported mass flow is not constant, indicating increased errors in the measurements and data processing. It is believed that the errors relate to the area-weighted averaging of velocities in combination with blockages and stratification, jet fan influences, and radiation effects on the temperatures used to calculate velocity from the pitot probes.

Jet fans were running just upstream of Loops 209 and 207. Figure 1 suggests that Loops 209 and 207 were affected by those jet fans. Mass flow estimation at Loops 304 and 302 appears to be influenced by temperature effects. Beneath the plot of the flow rates, the temperature

contour plot of the corresponding test, extracted from the test report [5], shows that upstream mass flow anomalies were not due to backlayering (826.5 s after ignition).

The difficulties with interpreting these data precisely led to temperature readings from the tests being the comparison basis for CFD validation. While they are still subject to radiation close to the fire, they are not sensitive to stratification, area-weighted averaging, or jet fans.

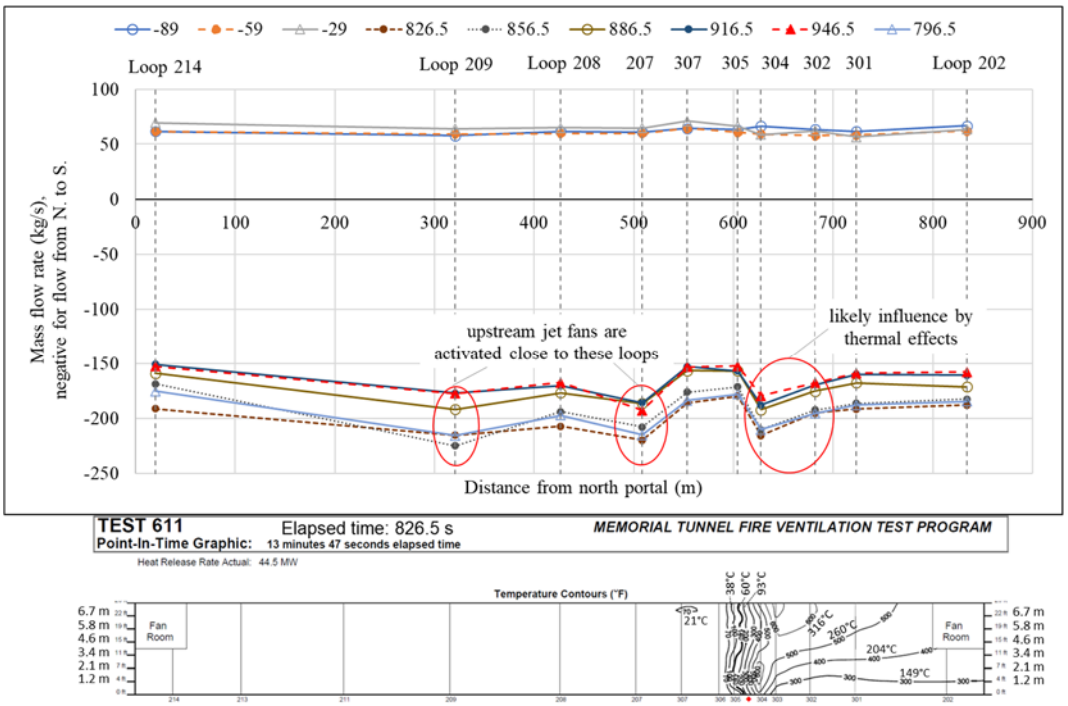

Figure 1: The upper plot shows mass flow rate at different measurement loops prior to ignition (89 s, 59 s and 29 s prior to ignition, all above the axis) and for several time stamps after ignition (826.5 s to 976.5 s after ignition) for test 611 (50 MW pan fire). The lower plot depicts the temperature contours at 826.5 s after ignition, to illustrate the smoke propagation at that time [5], [6].

To validate the CFD model for low as well as high fire heat release rates (HRR), pan fire tests with HRRs of 10 MW, 50 MW and 100 MW were selected. The essential case parameters are listed in Table 1. The flow parameters listed are averages over a period when the flow and smoke layer were fairly constant. This allows the comparison of the measured values with a steady-state simulation in a reasonable way.

Table 1. Input and test parameters extracted from the Memorial Tunnel test data [5], [6], [7]for three validation cases. Bulk temperatures are mass-averaged temperatures.

Parameter	Case 1	Case 2 (base)	Case 3
Test number	606A	610	615B
Elapsed time used for averaging (sec.)	1651 to 1680.5	191.5 to 281	678.5 to 828.5
Measured total HRR[1](MW)	11.1	54.3	104.6
Activated jet fan/s	JF3	JF2, 5, 8, 11 & 14	JF1, 3, 4, 6, 7 & 9
Fire pan/s used, according to Figure 2	10 MW	50 MW	50, 30 & 20 MW
Flow rate - Loop 214 (m^3/s)	143.2	148.3	139.8
Average velocity - Loop 305 (m/s)	2.92	3.00	2.85
Blockage area at Loop 305[3] (m^2) [5], [7]	10.2	10.2	10.2
Free tunnel cross sectional area (m^2)	59.9	59.9	59.9
Average velocity unobstructed tunnel section (m/s)	2.44	2.51	2.38
Upstream temperature - Loop 214 (°C)	3.6	4.0	6.8
Upstream temperature - Loop 207 (°C)	8.5	7.3	12.0
Upstream temperature - Loop 307 (°C)	9.0	7.2	14.8

Measured bulk temperature after fire - Loop 302 (°C)	53	190	451
Measured bulk temperature after fire - Loop 303 (°C)	57	217	475
Upstream density - Loop 214 (kg/m³)	1.28	1.27	1.26
Specific heat capacity (kJ/kgK)	1.014	1.044	1.096
Theoretical bulk temperature after the fire based on total HRR(°C)	69	282	554
Radiative fraction[2] (-)	0.21	0.24	0.17

[1] Measured heat release rate corrected by the CO to CO_2 ratio to account for non-ideal combustion [5], [6]
[2] Ratio between measured bulk temperature and the theoretical bulk temperature rise resulting from the total HRR is assumed to be the radiative fraction.
[3] Value as stated in Section 8.8.4 in the comprehensive test report [5], and in the paper from Kile&Gonzalez [7]. The fraction of the tunnel area blocked is about 17%, as also reported in the same references.

3. CFD MODEL

The CFD validation was carried out by using the simulation software ANSYS Fluent version 2021 R1 [8], [9], [10]. During the validation process, a fire test with a nominal fire heat release rate of 50 MW was chosen as the base case (Case 2 in Table 1) and analysed with two different common approaches as to how the fire is represented in the numerical model. The two methods for representing the fire are "volumetric heat source" and "simulation of the combustion process" and explained in more detail in Section 3.2.

To validate against a wide range of fire sizes, the fire representation with the most promising results was also applied to simulating 10 MW and 100 MW fire tests.

As a final step and comparison, the base case validation (50 MW) was also analysed with FDS (Fire Dynamic Simulator version 6.7.1) [11], as outlined in Sections 4 and 5.3.

3.1. Geometry and Computational Mesh

Geometric parameters were mainly extracted from the test reports [5], [6] to create a detailed model of the Memorial Tunnel including the jet fans, fire pans, measurement loops and measurement equipment/data acquisition units obstructing part of the tunnel cross section around the loops. Setup sketches and test notes made at the time were also provided by [12], to assist in reproducing the size and position of the data acquisition, measurement units, and instrument loops. Unfortunately, the sketches were made when the false ceiling was still in place. However, it has been confirmed that the position and size of the recorded obstacles were similar after the ceiling was removed [12]. Also, the reconstruction of the geometry based on photos and those sketches confirmed the obstruction area as being 10.2 m² at Loop 305. As a figure of 110 ft² (10.2 m^2) is noted for Loop 305 in the test reports [5] and [7]. This is important, since the average air velocity at Loop 305 (11.3 m upstream of the fire site centre-line) was used as the measure for the critical velocity (about 20% higher than the unobstructed upstream average velocity [5], [7]). In the Memorial Tunnel report, slightly different cross sectional areas are stated, ranging from 59.6 m^2 to 60.4 m^2. The replication of the tunnel geometry based on the plotted tunnel profile with detailed dimensions, as depicted in Figure 2, resulted in a cross-sectional area of 59.91 m^2, which is in the quoted range, has a basis in the records, and was therefore adopted. At the portal sections, the northern and southern central fan rooms limit the ceiling height so that the cross-sectional area reduces to 37.1 m^2. The position and size of the fire pans was incorporated as shown in Figure 2. In total, 24 jet fans, each with a flow rate of 42.95 m^3/s and a discharge velocity of 34.2 m/s were installed in banks of three upstream and downstream of the fire, as depicted in Figure 3. Jet fans influence the velocity profile and turbulence in the tunnel and so the operating jet fans were also implemented in the CFD model. The groups of jet fans downstream of the fire were installed in a later stage of the tests and were not relevant to include in the model for the tests analysed. The total tunnel length from portal to portal is 853.75 m. Location of the measurement loops, as well as of the individual sensors in the tunnel profile, are illustrated in Figure 3.

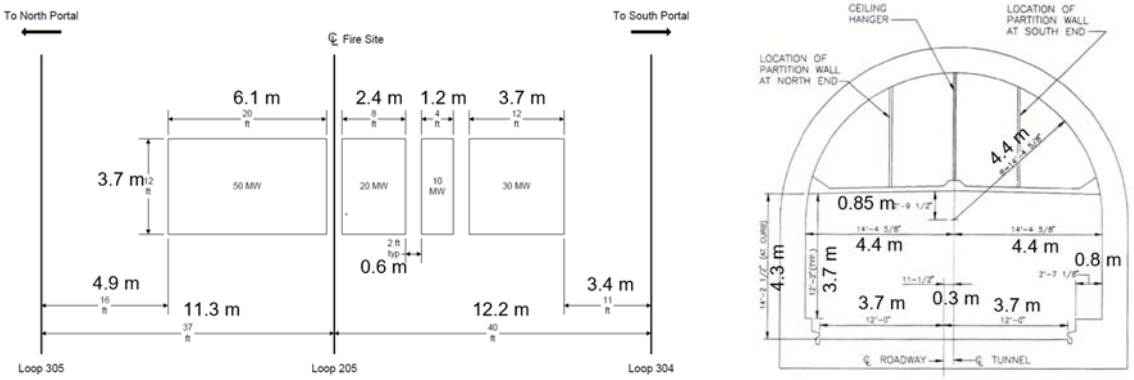

(**a**) (**b**)

Figure 2. Sketches from the Memorial Tunnel report [5], [6].
(**a**) Configuration and dimensions of the fire pans used, which were set about 0.76 m above the tunnel floor; (**b**) Memorial Tunnel cross-section with dimensions (looking north).

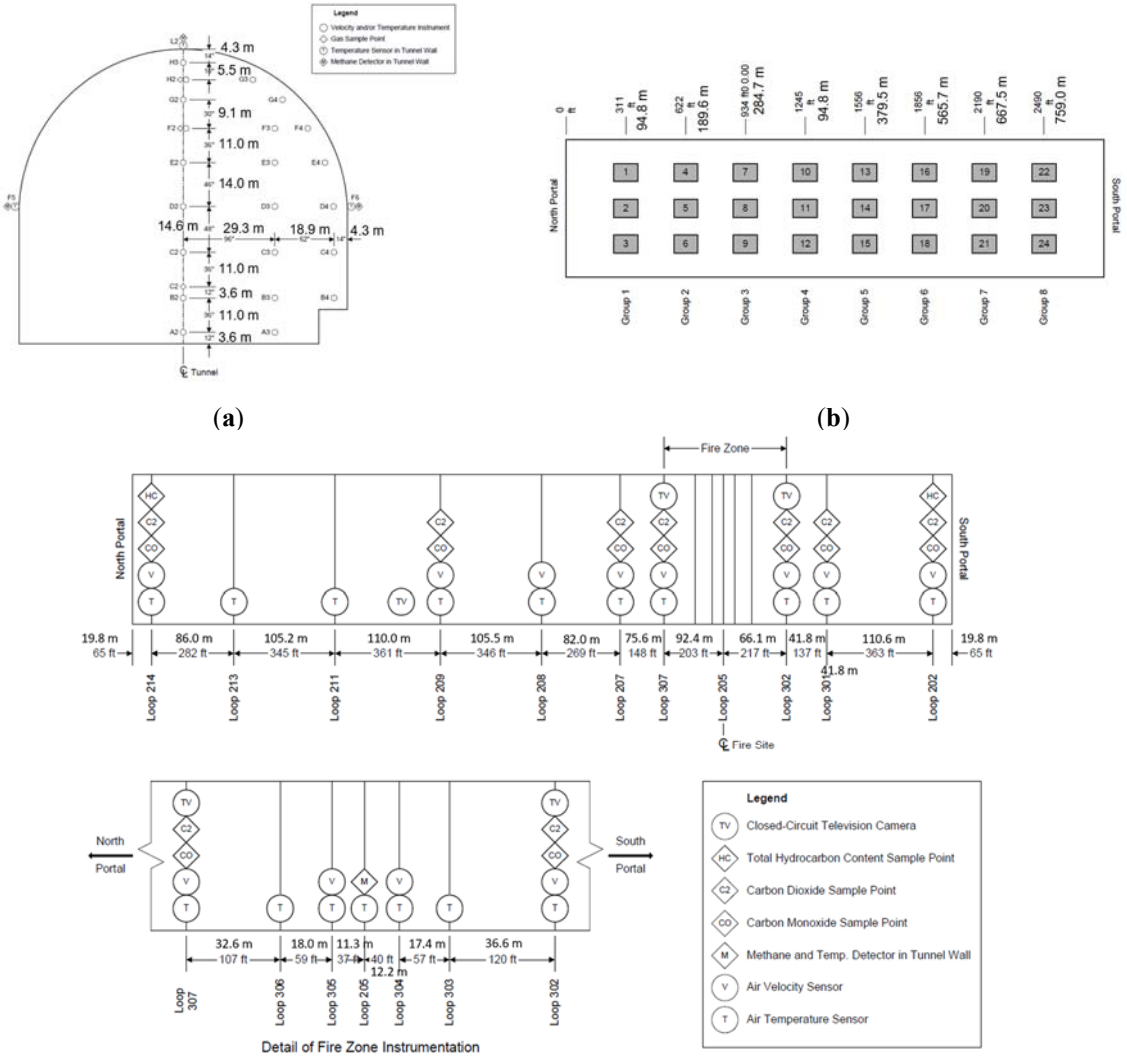

(**c**)

Figure 3. Sketches from the Memorial Tunnel report [5], [6].
(**a**) Location of the different sensors at the measurement loops (looking north);
(**b**) Location and description of the jet fan groups throughout the tunnel. Jet fans 16 to 24 were installed at a later stage of the tests and are not relevant for the cases considered.
(**c**) Instrument loop locations, with instrument types at each loop.

The whole domain was meshed with polyhedral surface elements in combination with hexahedral-core elements. To resolve the boundary layer at the walls, prism elements were created at the solid surfaces (fire pan, instrumentation tree, jet fans etc.). The element size within 40 m of the fire pans ranges from 0.02 to 0.1 m. Beyond the fire location, the elements grow to approximately 0.3 m. For the jets downstream of the jet fans, a finer mesh with a maximum element size of 0.1 m was introduced by means of a conical body of influence. The whole domain was meshed with approximately 35 M numerical elements. Figure 4 depicts the computational mesh around the fire pans (**a**) and jet fans (**b**).

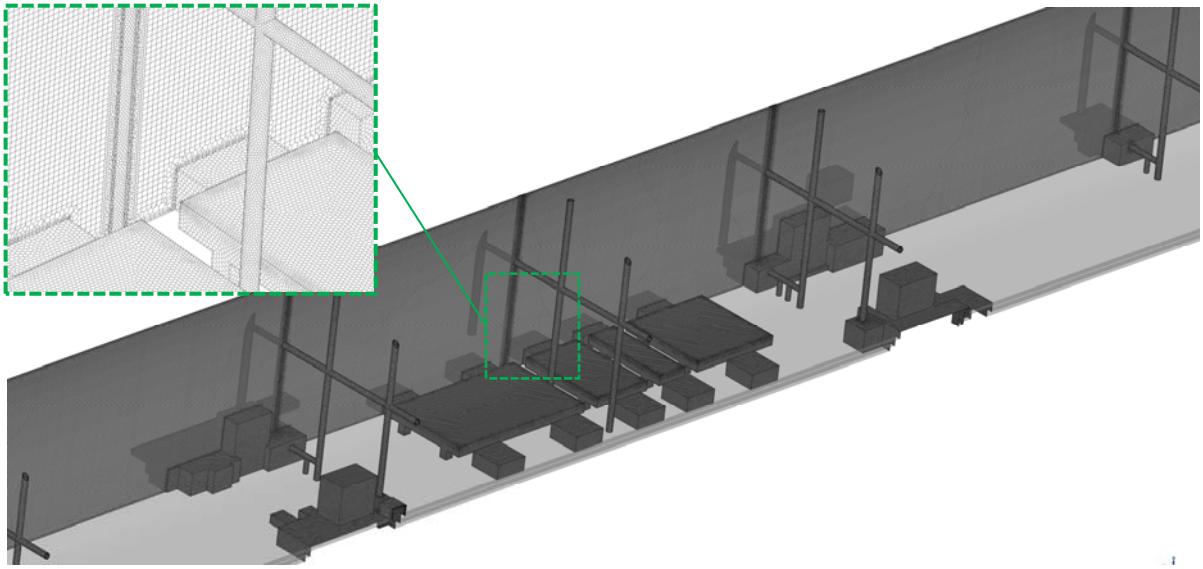

(**a**)

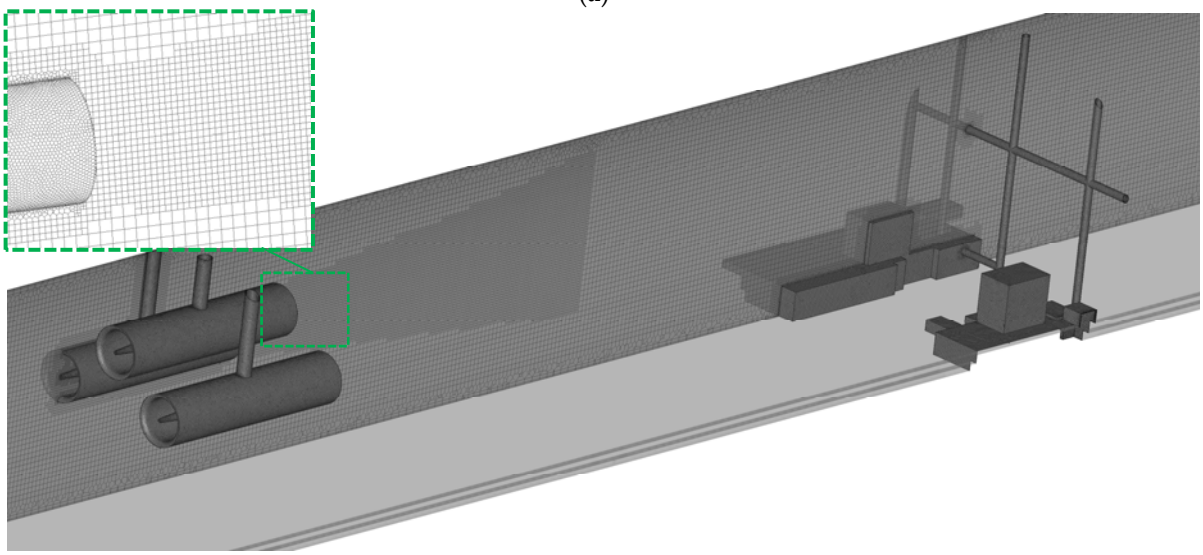

(**b**)

Figure 4. Computational mesh: (**a**) around the fire pans; (**b**) around jet fan group 5 and Loop 207.

3.2. Simulation Procedure and Methodology

Simulations were carried out in ANSYS Fluent using a pressure based, steady-state, Reynolds-averaged Navier-Stokes (RANS) solver with a spatial discretisation method of 2nd order. The realizable k-ε model with scalable wall function was applied. This turbulence model was developed to more accurately predict the spreading rate of planar and round jets and provides a good performance for flows involving rotation, boundary layers under strong adverse pressure gradients, separation and recirculation [8], [9]. The turbulence model was selected due to the

expected flow behaviour (jet flow at jet fans as well as separation and recirculation around the instrument trees), for its robust and efficient performance, and its accuracy. Buoyancy effects of the smoke are fully considered by using the incompressible ideal gas law. The fire is commonly represented with two different approaches as already noted at the beginning of Section 3, and further described below. Both have been tested and compared for test 610 which is a 50 MW pan fire (Case 2 in Table 1).

Volumetric heat source: The fire is represented as a source of heat and mass without simulating the combustion process, as proposed in [13]. In that approach, the heat release rate due to combustion is simplified as a volumetric heat source in an adopted fire region. As the heat is released in that region, the generated temperature depends not only on the heat release rate, but also on the size and definition of the pre-defined volume. This is essentially giving the model information on the flame size and shape, and the distribution of the release of heat. Of course, the size and shape of the flame are not known beforehand, and should be results of the model, not inputs, and so the volumetric heat source approach is adding assumptions that may not represent the real situation. For this validation, different (rectangular prism) heat source dimensions were analysed, and compared with the test results. The fuel mass due to combustion is considered in an additional mass source term in the continuity equations.

Eddy-dissipation combustion model: The combustion process is calculated by means of a turbulence-chemistry interaction model based on the work of Magnussen and Hjertager [14]. The chemical reaction rate is controlled by turbulent mixing and shows an acceptable performance for pool fires as suggested in [15]. Owing to the absence of detailed information on the combustion reaction, an ideal stoichiometric combustion was adopted. To reflect the Memorial Tunnel fire tests, a fuel oil with a chemical formula of $C_{19}H_{30}$ was introduced as fuel vapor coming from the pan surface.

Thermal radiation was not simulated for either the volumetric heat source or the eddy-dissipation combustion model. Instead, a radiative fraction approach as explained in [13] has been adopted, capturing the loss of thermal energy in a gross sense. This approach assumes that the radiative fraction of the total fire heat release rate is lost to the surroundings without affecting the temperature distribution within the tunnel. Particularly in the early stages of any fire, that is a reasonable approximation. The remaining energy heats up the air as it mixes with the plume. The radiative fraction of the individual test cases was estimated by the measured fire heat release rate and the bulk temperature downstream of the fire (see Table 1). The heat release rates during the Memorial Tunnel tests were measured through the fuel flow rate of the fuel supply pipe and the mass change of the fire pan. To account for the combustion efficiency, the HRR was corrected by the CO to CO_2 ratio. The corrected HRR as listed in Table 1 was used for the assessment. For the eddy-dissipation combustion model, a controller was implemented in the simulation, to adjust the fuel mass flow in such a way that the convective heat is achieved and maintained throughout the simulation.

The assumption of ideal combustion, and the radiative fraction approach, both require incorporation of an additional mass source. The simulation allowed for the additional mass source, adjusted to be appropriate to the real/factual fuel mass flow.

As already discussed in Section 2, Loop 214 (see Figure 3) gave the most reliable flow measurement during the tests. Tunnel air mass flow rate as the inlet boundary condition at the northern portal was determined based on the measured flow rate and bulk temperature at Loop 214. The air temperature measured just upstream of the fire was usually a few degrees higher than at the portal. This is caused by the tunnel wall temperature being higher than the ambient air temperature outside the tunnel. In order to have the right temperature and velocity just upstream of the fire, the mass flow at the northern portal was calculated based on the volume flow rate and density (bulk temperature) at Loop 214, but introduced into the tunnel

with the higher temperature that was measured just upstream of the fire (~Loop 208). The wall temperature was taken to be similar to the tunnel air temperature just upstream of the fire. The same approach was used for all simulation cases.

A piecewise-polynomial function for the temperature dependent specific heat capacity for the individual species was considered. The thermal dependency of the thermal conductivity and the dynamic viscosity for the individual species were estimated based on Sutherland's law with three coefficients, in combination with a mass-weighted mixing law.

4. FDS – SIMULATION PARAMETERS

For comparison with the Fluent validation, an FDS (version 6.7.1) simulation has been carried out with a 50 MW fire only (Case 2 as defined in Table 1). The geometry used for the ANSYS Fluent simulations (as described in Section 3.1) was exported as an STL file and imported into FDS via PyroSim (Revision 2020.1.0324). For the mesh, a cell size of 0.1 m x 0.1 m in the tunnel cross section, and 0.2 m longitudinally, was used. In FDS, stepwise representation of curved geometries makes it difficult to match the area precisely, such that either the velocity or the flow rate will be in error. The inlet boundary condition at the northern portal was a velocity inlet as the right tunnel air velocity is essential for reproducing smoke propagation upstream of a tunnel fire. For the southern (downstream) portal, a default open boundary condition was used. The fire in FDS is represented as a Simple Chemistry Reaction with a fuel-oil composed as $C_{19}H_{30}$ with the fire surface area sitting on the top of the 50 MW fire pan (see Figure 2 and Figure 5). Fire and flow parameters are applied as listed in Table 1 (Case 2). Turbulence in FDS was simulated with VLES (Very Large Eddy Simulation). The assumptions on the thermal radiation and the thermal conditions of the tunnel wall, were the same as discussed in Section 3.2. Jet fans are considered via an HVAC boundary condition with the flow rate as given in Section 3.1. Solver parameters like relaxation factor and velocity tolerance were adjusted to stabilize the numerical simulation and increase the accuracy of the pressure solver.

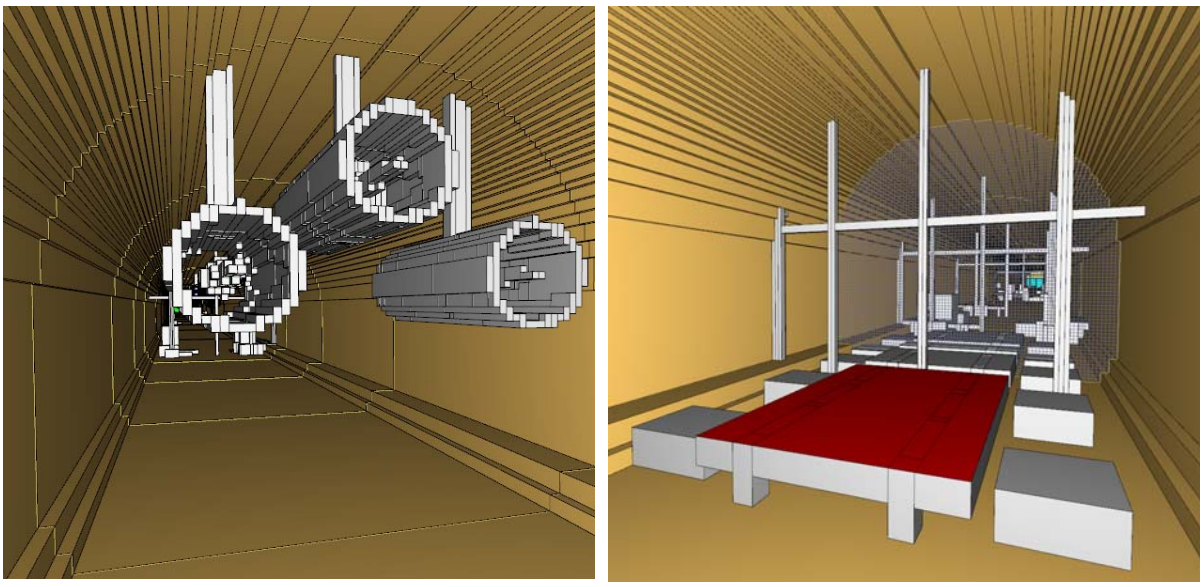

(**a**) (**b**)

Figure 5. Representation of the tunnel geometry in FDS with a cell size of 0.1 x 0.1 x 0.2 m. (**a**) Jet fan group 5, looking north. (**b**) Fire pans at Loop 205, looking south.

The FDS simulation encompasses a mesh of 17 million cells and was run on 128 cores over 3 weeks until it reached nearly steady state conditions. Even if this is considered as an upper limit of a practical usability, the curvatures of the geometry are still not resolved in an accurate way, due to the meshing limitations in FDS. Accurate representation of the geometry is important for resolving boundary and shear layers adjacent to the wall, as well as representing

the correct flow rate vs. velocity through the tunnel or jet fan. All of that is regarded as essential for an accurate prediction of smoke propagation upstream of a fire.

5. RESULTS OF THE VALIDATION AND DISCUSSION

For all simulated validation cases, Figure 6 to Figure 11 compare the bulk temperature along the tunnel axis and the temperature profiles over the tunnel height against the corresponding test results [5] and [6]. Thermocouple readings at a given elevation are averaged in the temperature profiles at the different measurement loops. The representative elevation area is a horizontal slice of the tunnel cross-section around the elevation instruments as specified in [5] and [6]. Identical horizontal slices have been used for evaluating the CFD simulations. For a better understanding of the temperature profiles, a contour plot of the temperature through the middle of the tunnel around the vicinity of the fire is also given for each case.

The higher bulk temperature seen in the test data at loops 205, 304, and 303 (close to the fire source) in the plots with the bulk temperature along the tunnel, is believed to be related to the impact of the thermal radiation on the temperature readings, as noted in [5] and [6].

5.1. Fluent - Volumetric Heat Source

The volumetric heat source approach was first analysed for a 50 MW fire on a more simplified model with a reduced length of tunnel modelled. Obstacles were only considered in the vicinity of the fire at the Loop 305. 205 and 304 and the influence of jet fans on the velocity profile was also neglected. Fire and input parameters are based on Case 2 as given in Table 1. The simplified model was used to more rapidly analyse and understand the effect of different heat source sizes. The objective of this part of the study was to understand which volumetric heat source definition would replicate the smoke stratification and temperature distribution most accurately. The heat source was placed directly above the 50 MW fire pan (see Figure 2, left), and the volume was varied by changing the height from 2 m to 2.6 m and 3.0 m. That correspondents to volumetric heat sources of 1.22 MW/m^3, 0.94 MW/m^3 and 0.81 MW/m^3, respectively. To quantify the impact of the simplification (neglecting jet fans etc.), the simulation with the 3.0 m heat source was repeated with all relevant details implemented.

Figure 6 compares the test temperature profiles at the individual instrument loops, against the results of the CFD simulations with the different heat source definitions. The plot below the temperature profiles compares the bulk temperatures along the tunnel axis. A contour plot of the temperature through the middle of the tunnel shows the temperature stratification, and gives an indication of the upstream propagation of the hot smoke.

Looking at the test result, the slight temperature increase at the upper part of Loop 305 indicates that the tip of the backlayering was close to Loop 305 but did not reach Loop 306 further upstream.

In all cases, the extent of the backlayering was not predicted very accurately, with backlayering over-predicted. Backlayering propensity also depends strongly on the definition of the volumetric heat source. The best result in terms of the backlayering prediction were with the 2.6 m high heat source, but the temperature tends to be more stratified than observed in the tests, with higher flow and temperature along the ceiling (less mixing between smoke and air). The latter applies to all cases analysed. Further cases with heat source heights of 1.8 m, 3.5 m and 4.5 m were also analysed, but the predicted backlayering length with the smaller and bigger heat source volumes was higher still (further discussion on the more likely position of the backlayering at that time of the selected test period is provided in Section 5.2).

The detailed simulation with the complete tunnel section, all jet fans and obstacles implemented did improve the prediction of the upstream smoke propagation but did not improve the accuracy of the temperature distribution downstream (see Figure 7).

The volumetric heat source approach is usually very economical, and a robust method to simulate tunnel fires, and is therefore often preferred. However, there is no inherent fire volume definition for any scenario, and as the smoke propagation and temperature distribution strongly depend on the heat source dimensions, this approach is not recommended for analysing confinement or critical velocity in a reliable way.

Heat source height of 2.0 m

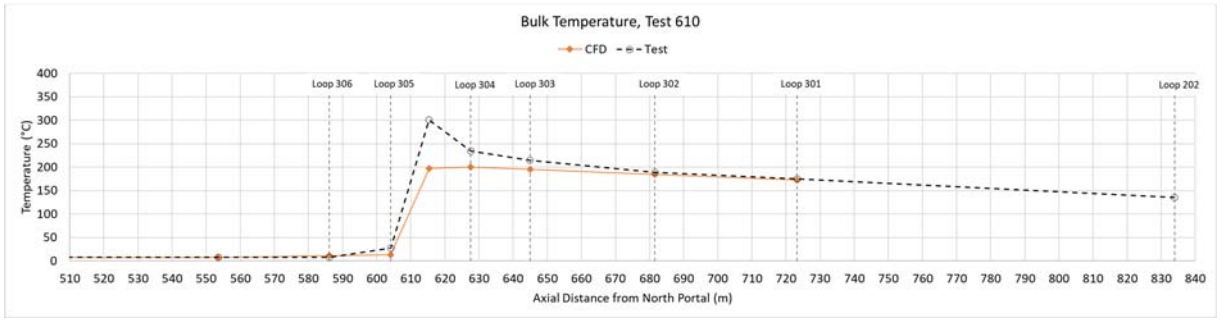

(**a**)

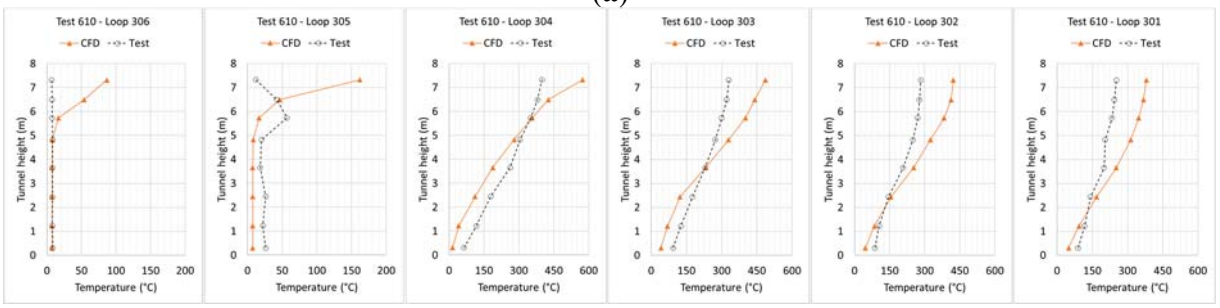

(**b**)

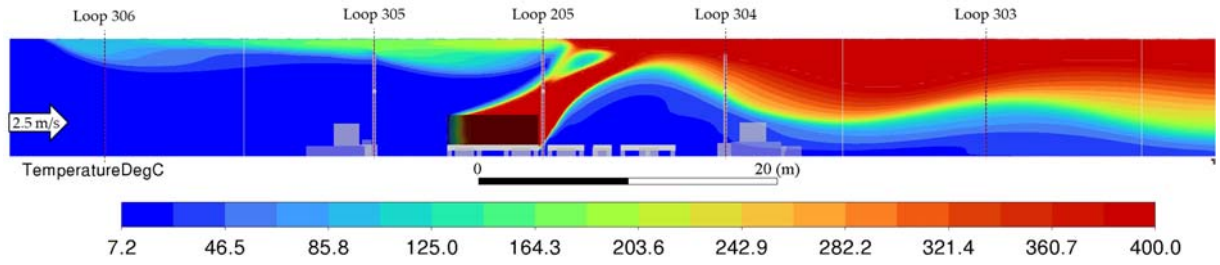

(**c**)

Heat source height of 2.6 m

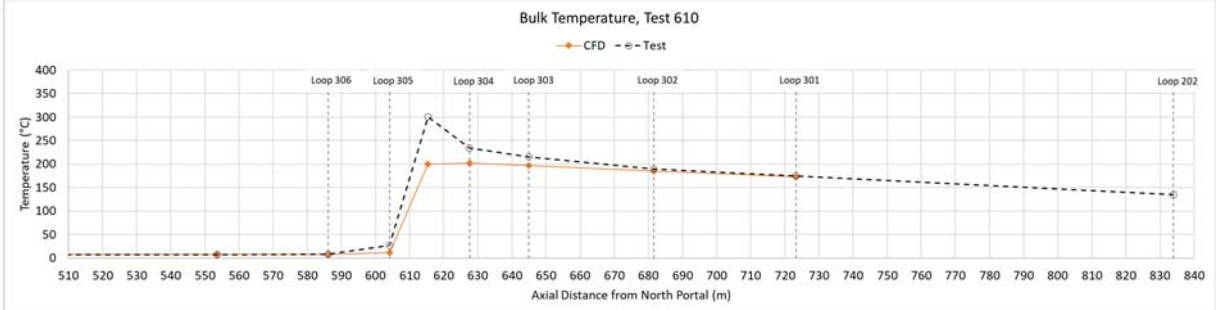

(**d**)

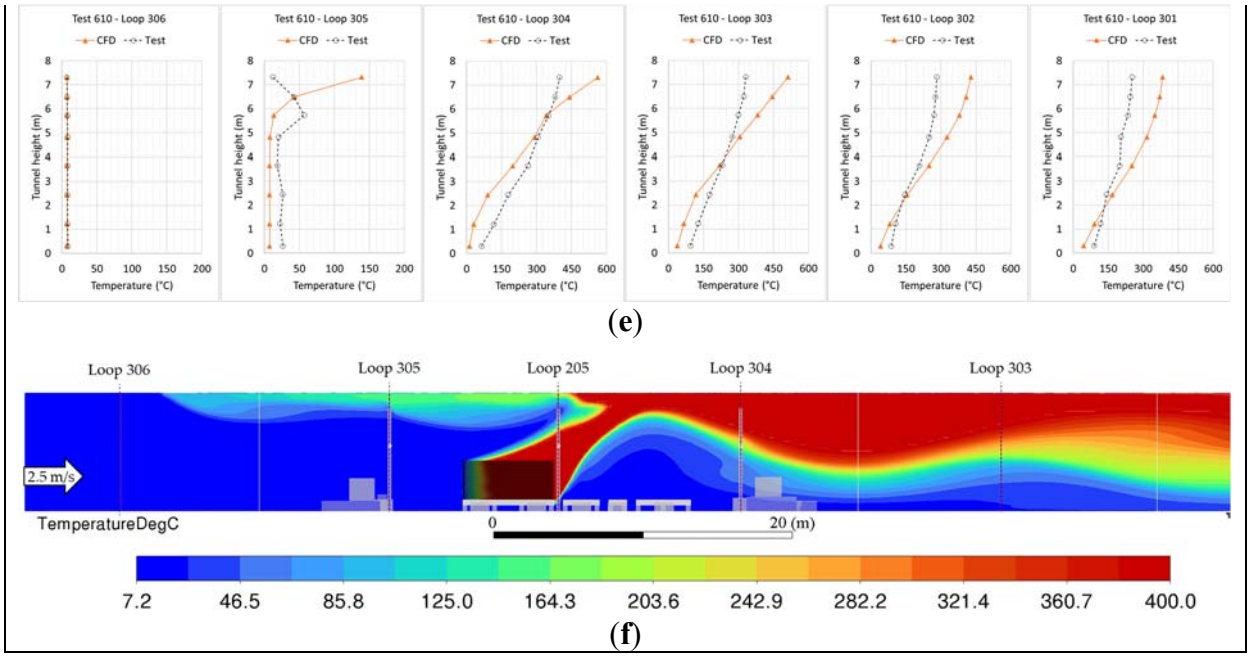

(**e**)

(**f**)

Heat source height of 3.0 m

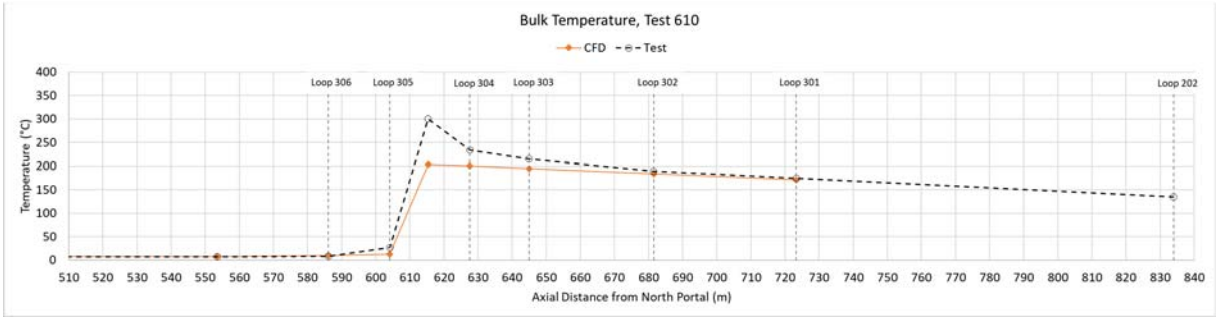

(**g**)

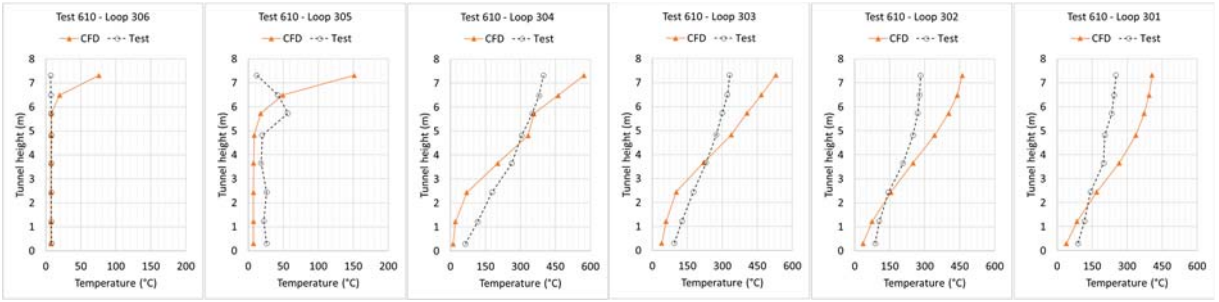

(**h**)

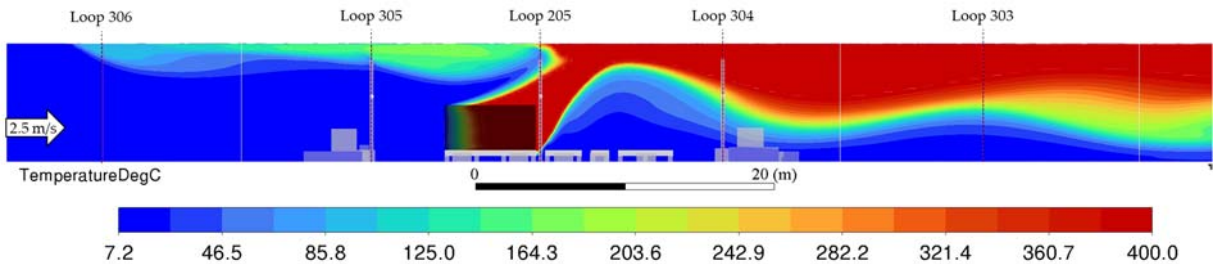

(**i**)

Figure 6. 50 MW validation (Case 2 from Table 1) with volumetric heat source. Comparison of simulation results with test results for test 610: (**a**), (**d**) and (**g**) Bulk temperature along the tunnel axis for different heat source heights, (**b**), (**e**) and (**h**) Temperature profiles over the tunnel height for

different loops in the vicinity of the fire and for different heights of the heat source, (**c**), (**f**) and (**i**) Contour plot of the temperature in °C through the middle of the tunnel and fire pans, for different heat source heights. Temperature is clipped to 400°C for a better visualisation of the temperature layering.

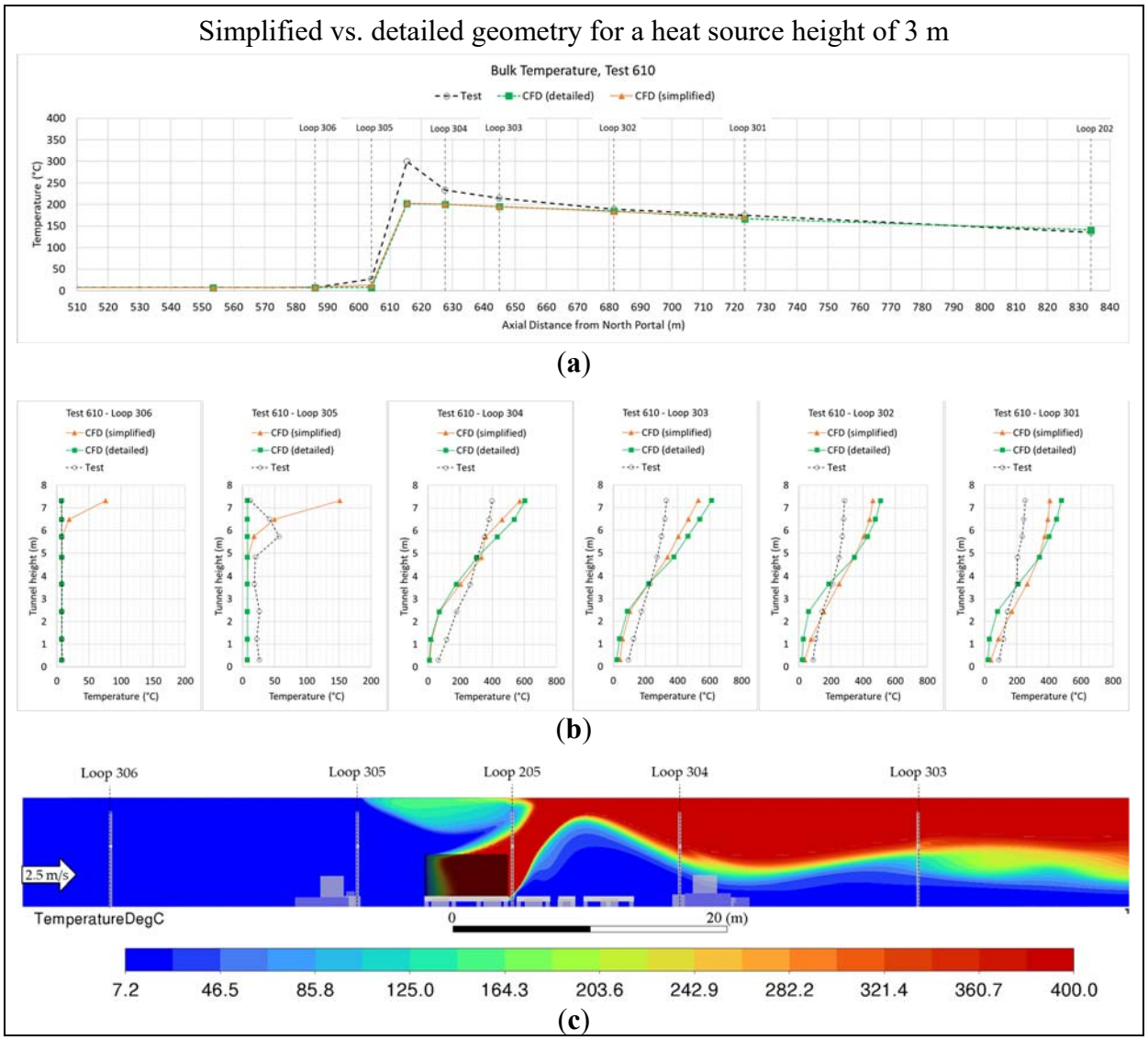

Figure 7. 50 MW validation (Case 2 from Table 1) with volumetric heat source height of 3.0 m. Comparison of: simulation results with simplified geometry; with detailed geometry; and the test results for test 610. (**a**) Bulk temperature along the tunnel axis, (**b**) Temperature profiles over the tunnel height for different loops in the vicinity of the fire, (**c**) Contour plot of the temperature in °C through the middle of the tunnel and fire pans. Temperature is clipped to 400°C for a better visualisation of the temperature layering.

5.2. Fluent - Eddy Dissipation Combustion Model

The simulation with the eddy-dissipation combustion model was carried out for all three validation cases listed in Table 1. Results of the temperature distribution along the tunnel and the temperature profiles at the different loops are presented in Figure 8 to Figure 10 for the three different fire cases.

In all cases, the temperature profiles downstream of the fire were predicted with reasonable accuracy. The higher temperature readings of the test data at the upper part of the temperature

profile close to the fire (Loops 304 and 303) might be related to the influence of thermal radiation on the sensors (see Figure 8 and Figure 9).

Besides the deviation of the bulk temperature close to the fire (influence due to thermal radiation on the temperature sensors during the tests), the bulk temperature at Loop 202 also shows a slight deviation, especially at higher downstream temperatures (higher HRR). Loop 202 is located in the smaller cross section near the south portal, with the reduced ceiling height. The step change in the cross-section area is just 1.5 m upstream of Loop 202. This step will have created a separation zone and recirculation close to the ceiling. The difference in bulk temperature seen at Loop 202 may be related to the difficulty in turning point measurements of velocity and temperature into bulk averages, for such a non-uniform flow.

The velocity in the tunnel during the Memorial Tunnel tests was adjusted using the jet fans installed in the tunnel upstream of the fire. These jet fans were not speed controlled. To change the air speed in the tunnel, a jet fan could be switched on or off, making the speed control fairly coarse. The buoyancy force and flow resistance of the 10 MW fire are quite low, certainly much lower than for a 50 MW or 100 MW fire. With the coarse control on jet fan forcing, the low resistance made it difficult to achieve a steady velocity where backlayering was just prevented. For the tests with low heat release rates, two active jet fans were insufficient to stop smoke propagation upstream of the fire, and three jet fans were too strong, so that the approaching air velocity was higher than required for preventing backlayering. The point at which backlayering was just prevented was analysed during the velocity change after turning the third jet fan on or off. This made it difficult to accurately determine the critical velocity for low heat release rates. The scatter in the reported data at low HRR reflects this.

The flow record simulated for test 606A (11.1 MW) was approximately 28 minutes after ignition, when the third jet fan was activated. Before that, smoke was propagating upstream of the fire so that the tops of Loops 304, 305, and partly 306, were covered in smoke for more than 15 minutes. When the smoke went back towards the fire site briefly (for around 2 minutes), the temperature readings show slightly increased values (Figure 8) which may possibly be explained by the thermal inertia of the temperature sensors only recently out of the smoke layer.

Test 610 (54.3 MW) shows backlayering above the deflected flames and plume which stops at the front of the first fire pan, just downstream of Loop 305 (see Figure 9). The sensor temperature at Loop 305 might have been increased by thermal radiation, as the instrument tree is only 5 m upstream of the fire. Also, the backlayering was slowly moving forward and backward with slight fluctuations in the fire dynamics and local velocity during the test.

At the beginning of test 615B (104.6 MW), all jet fans were switched off and the smoke was propagating in both directions towards the portals. About 3 minutes after ignition, 6 jet fans (as listed in Table 1) were activated so that the smoke was slowly pushed back towards the fire site. After 10 minutes, the upstream tunnel section was free of smoke. The simulated flow record was at around 12 minutes after ignition, just before one of the six jet fans was turned off and the upstream smoke propagation started again. The simulation shows a backlayering of smoke which stops just upstream of Loop 305 (see Figure 7). Looking at the temporal variation in the original data, the increased temperature around the ceiling at Loop 306 could be related to heated sensors that had been subject to hot smoke for more than 10 minutes and having not yet reached equilibrium with the temperature of the fresh air. It is assumed that the sensor readings at the lower part of Loops 305 and 304 are influenced by thermal radiation. The test results indicate that the smoke downstream of the fire was more mixed than is predicted by the simulation.

Based on the observations above, and acknowledging a few uncertainties in the temperature readings, it can be concluded that the smoke propagation and temperature distribution can be predicted within a reasonable accuracy by the simulation techniques and procedures applied.

Most importantly for the present purpose, the smoke extent matches the tests very well for the same conditions. However, it is important to also check other parameters, to see that the critical velocity is not correct by an 'accident' of compensating errors that may not compensate each other in other scenarios. The temperature profiles away from radiation effects are also predicted quite well, giving confidence that the analysis is a reasonable representation of the plume and smoke layer dynamics. That is; the technique is a reasonable tool for exploring critical velocity, for cases not dissimilar to the validated cases.

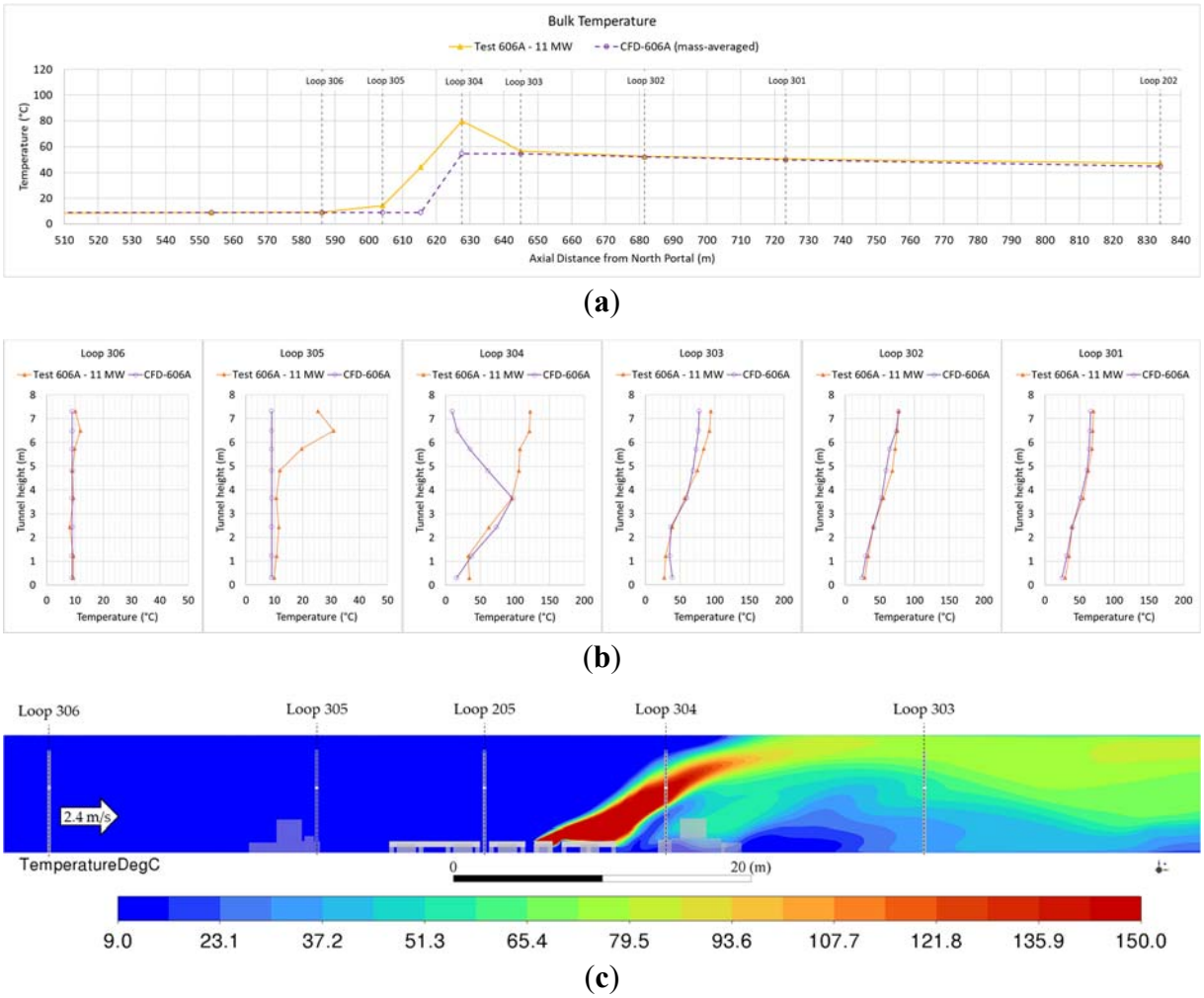

Figure 8. 11 MW validation (Case 1 from Table 1) with combustion model. Comparison of simulation results with test results for test 606A: (**a**) Bulk temperature along the tunnel axis, (**b**) Temperature profiles over the tunnel height for different loops in the vicinity of the fire, (**c**) Contour plot of the temperature in °C through the middle of the tunnel and fire pans. Temperature is clipped to 150°C for a better visualisation of the temperature layering.

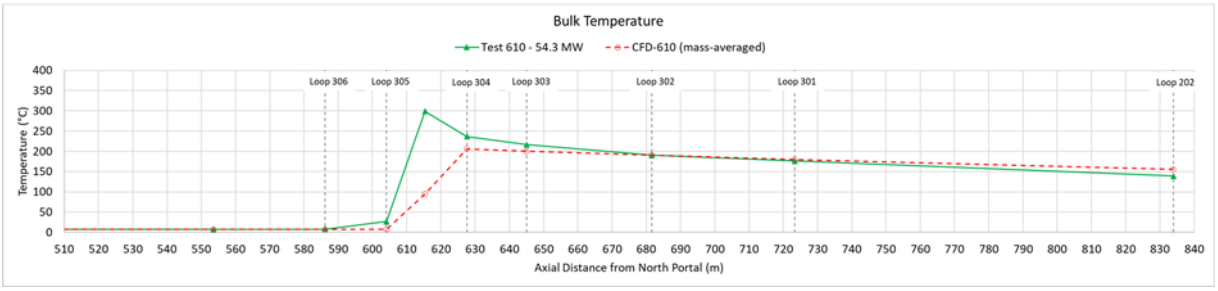

(**a**)

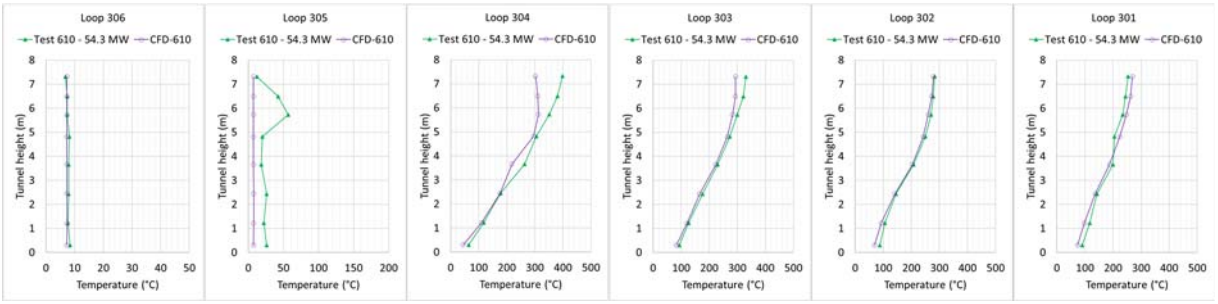

(**b**)

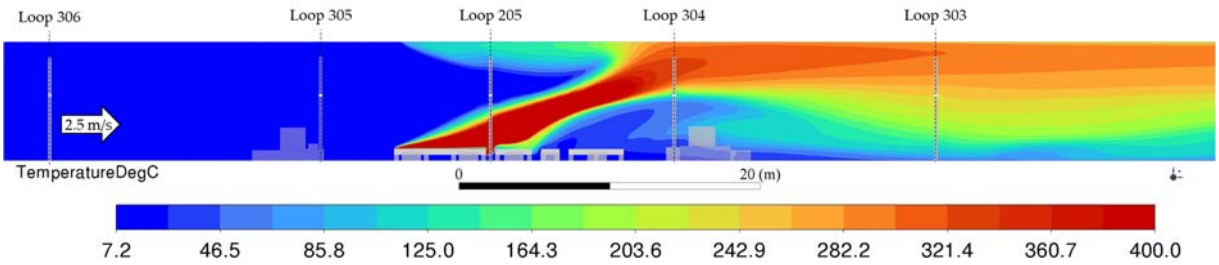

(**c**)

Figure 9. 54.3 MW validation (Case 2 from Table 1). Comparison of simulation results with test results for test 610: (**a**) Bulk temperature along the tunnel axis, (**b**) Temperature profiles over the tunnel height for different loops in the vicinity of the fire, (**c**) Contour plot of the temperature in °C through the middle of the tunnel and fire pans. Temperature is clipped to 400°C for a better visualisation of the temperature layering.

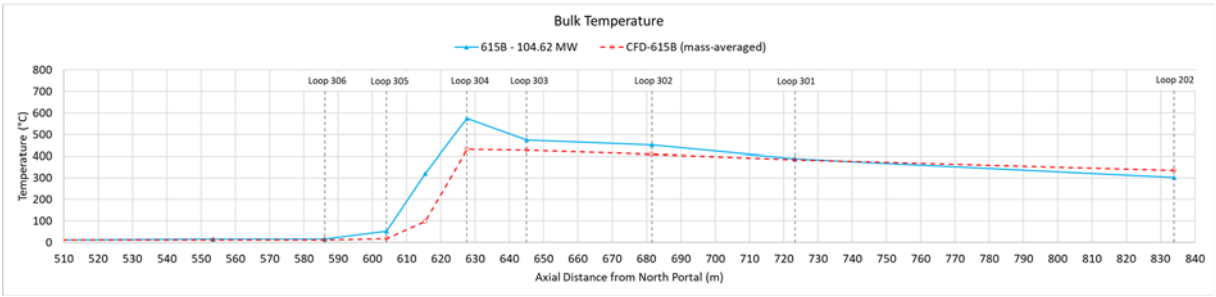

(**a**)

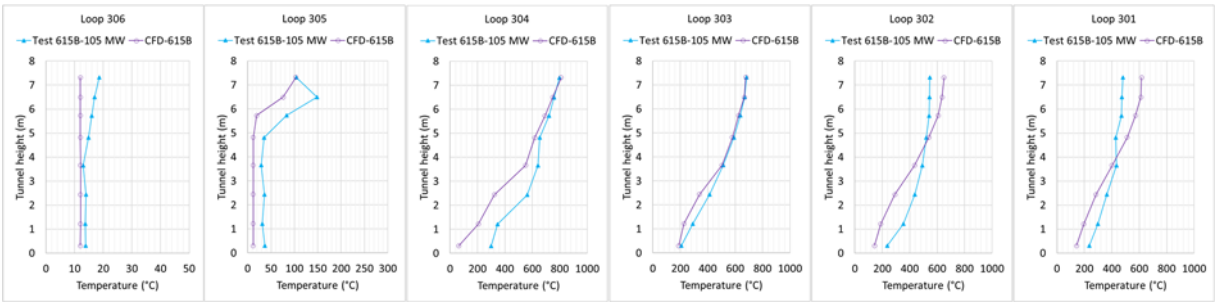

(**b**)

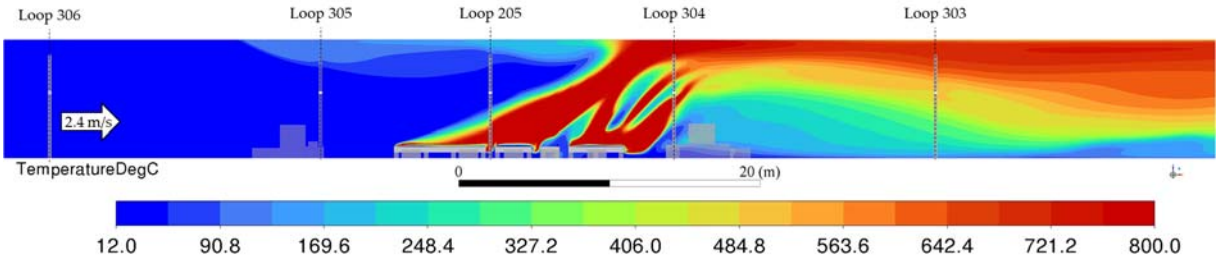

(**c**)

Figure 10. 105 MW validation (Case 3 from Table 1). Comparison of simulation results with test results for test 615B: (**a**) Bulk temperature along the tunnel axis, (**b**) Temperature profiles over the tunnel height for different loops in the vicinity of the fire, (**c**) Contour plot of the temperature in °C through the middle of the tunnel and fire pans. Temperature is clipped to 800°C for a better visualisation of the temperature layer.

5.3. FDS

The FDS simulation of Case 2 was run for 600 s. Smoke propagation was established and was almost steady state after 200 s. The values in the temperature profiles as illustrated in Figure 11 are averages over a period of 50 s, close to the end of the simulation. The FDS simulation predicts a smoke propagation upstream of the fire of approximately 360 m, whereas the simulation with the eddy-dissipation combustion model agrees with the test result, with almost no upstream smoke propagation for the 50 MW fire case. The FDS upstream smoke layer stops between Loops 207 and 307, as it is opposed by the running jet fans at JF-Group 5. Without the activated jet fans, the analysis of the simulation results indicates that the backlayering of hot smoke gases would propagate upstream even further. The temperature profile along the tunnel axis shows an increased bulk temperature upstream of the fire due to the upstream smoke layer. The bulk temperature at the southern portal (Loop 202) is missing in the plot as it has not been recorded during the FDS simulation. The comparison of the temperature profiles along the tunnel height shows that the smoke downstream of the fire is less mixed, which results in higher temperatures in the upper part of the tunnel and a more energetic smoke layer.

Based on these observations, it can be concluded that the smoke propagation and temperature distribution are not predicted within a reasonable accuracy by FDS and the applied simulation techniques. Analysing smoke propagation with FDS as described here would lead to overprediction of critical velocity or confinement velocity required for preventing or controlling backlayering.

The poor representation of surface curvatures in FDS compromises efforts to accurately resolve and predict the boundary layer adjacent to the wall, which might be one reason for the unsatisfying results in the smoke propagation. Analysing smoke propagation in straight and rectangular tunnels may potentially improve the results if the boundary layer adjacent to the wall is sufficiently resolved by adequate cell sizes and an appropriate wall function is used. However, caution regarding the accuracy of the flow and pressure field in FDS is required, as several issues with numerical oscillations in the pressure solver have been reported [16], [17] and [18].

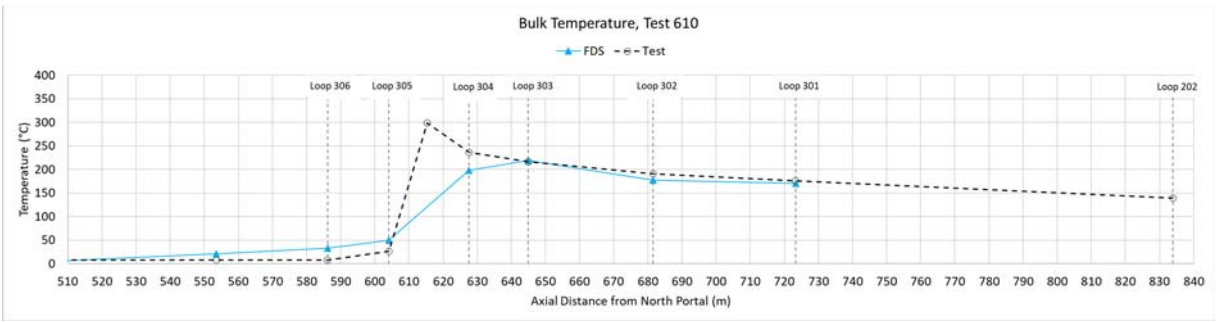

(**a**)

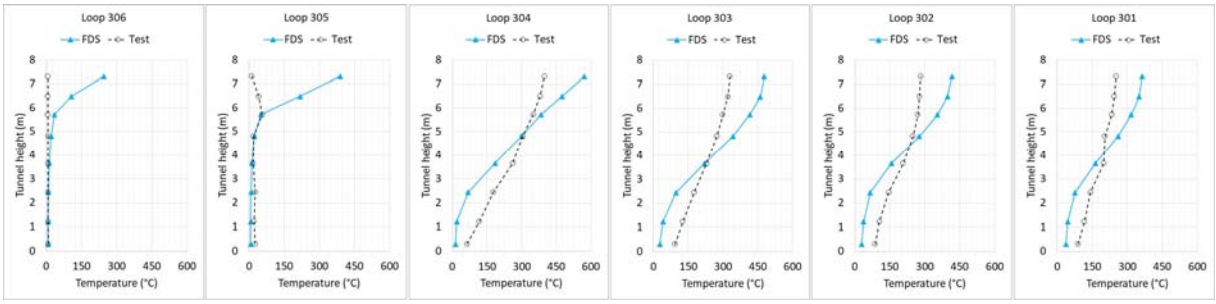

(**b**)

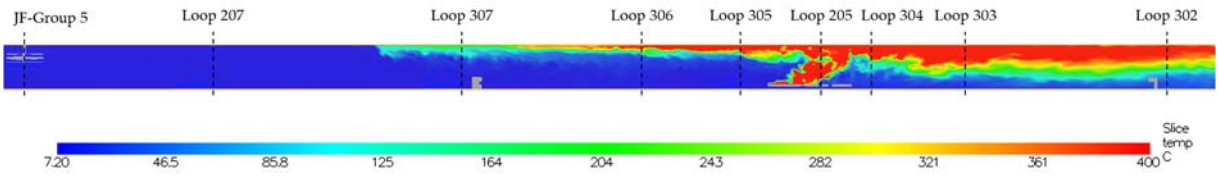

(**c**)

Figure 11. FDS simulation for 50 MW fire (Case 2 from Table 1) after reaching steady state conditions. Comparison of simulation results with test results for test 610: (**a**) Bulk temperature along the tunnel axis, (**b**) Temperature profiles over the tunnel height for different loops in the vicinity of the fire, (**c**) Contour plot of the temperature in °C through the middle of the tunnel and fire pans. Temperature is clipped to 400°C for a better visualisation of the temperature layering.

The current work finds that FDS is not predicting the flow field accurately for tunnel smoke control when applying reasonable parameters. A study for the U.S. Federal Highway Administration [19] explored simulation parameter variations that might bring FDS into some alignment with known data. Best agreement with the Memorial Tunnel test data was only

achieved by using a volumetric heat source, by making the mesh very coarse (0.4 m), and by using unrealistically large wall friction factors (Darcy Weisbach friction factor up to 0.183). Problems with volumetric heat sources are that the plume is artificially constrained, and the temperatures generated may not be real, as discussed earlier. Results from a coarse mesh cannot be relied on when the results vary strongly with mesh size as clearly demonstrated in [19]. When using reasonable parameters for wall friction and mesh size in FDS, the FHWA study [19] shows a considerable overprediction of backlayering. While the conclusions of the FHWA study imply some utility of FDS for tunnel smoke control when using unreasonable inputs, the detail presented supports the current findings. The FHWA work confirms in a more comprehensive way that, using credible simulation parameters, smoke propagation, temperature distribution, and the velocity needed for smoke control, are not predicted within a reasonable accuracy by FDS.

6. COMMENTARY AND CONCLUSION

In this CFD validation study, smoke propagation and temperature distributions for tunnel fires were analysed with different fire representations, and compared with the results from the Memorial Tunnel test program.

A volumetric heat source can predict the upstream smoke propagation with reasonable accuracy but provides a poor prediction of the temperature distribution downstream of the fire. However, the results are very sensitive to the heat source size. Without representing the whole flow field reasonably, agreement on backlayering may just result from ‘lucky’ tuning of an otherwise physically unrealistic approach. The volumetric heat source approach is not recommended as a reliable method.

The eddy-dissipation combustion model in Fluent represents the smoke propagation and temperature distribution with sufficient accuracy for small (10 MW) as well as big (100 MW) tunnel fires.

The results produced with FDS showed a clear overprediction of the upstream smoke propagation and also gave an unconvincing representation of the temperature distribution.

The complexity of the physics and the number of different flow regimes in the critical velocity and backlayering problem make reproduction by CFD very challenging. The answers can be very sensitive to input assumptions about which there is no ‘right’ answer (e.g. volumetric heat source size), and to modelling approaches, algorithms and coding (FDS, Fluent) as demonstrated here. Without a comparable validation case, the CFD cannot be relied on for design of tunnel smoke control.

The work done establishes a clear method for using CFD to design smoke control in the Memorial Tunnel. That is not directly useful, as the Memorial Tunnel is already designed, built, operated, de-commissioned, and tested for critical velocity. The question is how widely the above method can be applied to the design of new tunnels. The non-committal answer is that the method will be useful where the physics is sufficiently similar to that in the Memorial Tunnel tests. That probably means that is good for fires of 10 MW to 100 MW in all road tunnels designed for truck traffic (reasonably high clearance).

The validation was done for pool fires only. Whether the applied combustion technique can be stretched to other fire types e.g. solid fuel fires, fires with considerable obstructions, battery fires etc. might require further validation. Furthermore, the approach is for fires with a reasonable duration (approximately 20 to 30 minutes). Tunnel wall parameters would need to be re-evaluated when analysing smoke propagation for fires with a longer period than that. The same applies for tunnels with fire board on the walls or any other cover on the wall that limits

the heat transfer. Especially for analysing long-lasting fires, a transient simulation might be required to evaluate the influence of wall heating on the smoke propagation.

It is not clear that the smoke flow regimes in a wide tunnel are physically different to propagation of a smoke layer in a standard tunnel, such that a change in turbulence or combustion models would be called for. It seems likely that the CFD techniques presented here would have some usefulness for a very wide tunnel.

One case where some greater caution might be required is in tunnels where a ceiling velocity deficit is created by a proliferation of fittings (signs, lights, cable trays) above the traffic space. It seems possible that there could be unexpected interactions between smoke and a highly non-uniform velocity profile which requires an accurate representation of the vortices and turbulence induced.

The authors' view is that validation of the CFD system of (analyst + software + model choices) is likely to provide for a far better way of extrapolating from known test results to a particular tunnel, than is offered by any of the formulae past or present for critical velocity. There are no credible formulae for confinement velocity.

Conversely, unvalidated CFD can readily give either incorrect results, or for a more skilled analyst, whatever result the analyst wants. Unvalidated CFD should not be used for designing tunnel smoke control.

7. ACKNOWLEDGEMENTS

We thank Joe Gonzalez and Matthew Bilson for providing details and raw data of the Memorial Tunnel Fire Ventilation Test Program. That made it possible to have a better understanding of the test data.

8. REFERENCES

[1] A. Lönnermark, "On the characteristics of fires in tunnels," Dissertation, Department of Fire Safety Engineering, Lund University, Lund, Sweden, 2005.

[2] P. Sturm, M. Beyer and M. Rafiei, "On the problem of ventilation control in case of a tunnel fire event," *Case Studies in Fire safety, CSFS 22, Elsevier publishing, doi: 10.1016/j.csfs.2015.11.001,* 2015.

[3] M. Beyer, C. Stacey and A. Dix, "Critical velocity and tunnel smoke control Part 2, Filling the NFPA 502 void," *Australian Tunnelling Society,* p. 6, 2021.

[4] C. Stacey and M. Beyer, "Critical of critical velocity - An industry practioner's perspective," in *10th International Conference 'Tunnel Safety and Ventilation'*, Graz, 2020a.

[5] MTFVTP, "Memorial Tunnel Fire Ventilation Test Program - Comprehensive Test Report," Bechtel/Parsons Brinckerhoff, Boston, 1995a.

[6] MTFVTP, "Memorial Tunnel Fire Ventilation Test Program - Memorial Tunnel Test Data Report incl. 9 discs of raw data," Bechtel/Parsons Brinckerhoff, Boston, 1995b.

[7] G. W. Kile and J. A. Gonzalez, "The Memorial Tunnel Fire Ventilation Test Program: The Longitudinal and Natural Tests," *ASHRAE Transactions 103, ProQuest Science Journals,* p. 701, 1997.

[8] Ansys, Inc, “ANSYS Fluent User's Guide, Release Janury 2021 R1,” USA, 2021a.

[9] Ansys, Inc, “ANSYS Fluent Theory Guide, Release January 2021 R1,” USA, 2021b.

[10] Ansys, Inc, “ANSYS Fluid Dynamics Verification Manual, Release January 2021 R1,” USA, 2021c.

[11] K. McGrattan, S. Hostikka, R. McDermott, J. Floyd and M. Vanella, “Fire Dynamics Simulator User's Guide,” Natianal Institute of Standard and Technology, USA, 2013.

[12] J. Gonzalez and M. Bilson, *Private communication - Sketches of measurement loops and test notes,* 2020.

[13] K. Karki, S. Patankar, E. Rosenbluth and S. Levy, “CFD Modeler for Jet Fan Ventilation Systems,” in *BHR Group 10th ISAVVT*, Boston, USA, 2000.

[14] B. F. Magnussen and B. H. Hjertager, “On mathematical models of turbulent combustion with special emphasis on soot formation and combustion,” in *16th Symp. (Int'l.) on Combustion*, 1976.

[15] A. A. Attar, M. Pourmahdian and B. Anvaripour, “Experimental Study and CFD Simulation of Pool Fires,” *International Journal of Combustion Applications (0975 - 8887),* vol. Volume 70, no. No. 11, pp. 9-15, May 2013.

[16] C. Ang, G. Rein and J. Peiro, “Unexpected Oscillations in Fire Modelling Inside a Long Tunnel,” *Fire Technology,* no. 56, pp. 1937-1941, 2020.

[17] K. McGrattan and R. McDermott, “Response to "Unexpected Oscillations in Fire Modelling Inside a Long Tunnel" by Ang et al,” National Institute of Standards and Technology, Gaithersburg, Maryland, USA, 2022.

[18] I. Riess, “Fixed Fire Fighting Szstems and Tunnel Ventilation,” Riess Ingeneur-GmbH, Zürich, 2021.

[19] T. Warren, S. Bartha, M. Bilson, B. Conell and E. Persson, “Fixed Firefighting and Emergency Ventilation Szstems for Highway Tunnels - Computer Modeling Report,” U.S. Department of Transport, Federal Highway Administration, New York, 2022.